



Stability and deformation control of deep foundation pits of half covered excavation subway in soft soil

Jianpeng Qin¹, Jie Yuan^{1,*}, Xiang Xiao¹, and Yiheng Pan²

¹China Construction Infrastructure Co., Ltd., Beijing, 100044, China

²College of Harbour and Coastal Engineering, Jimei University, Xiamen, 361021, China

*Corresponding author's e-mail: cscic_yj@163.com

Abstract. A three-dimensional analysis model was established by finite element simulation to study the deformation and internal force changes of the cover plate, enclosure structure, support system, and surrounding soil during the excavation process of deep foundation pit at the Tatou Station of Fuzhou Metro Line 4 in soft soil. A corresponding theoretical basis for the excavation and support of the foundation pit project was provided. It was found that the maximum horizontal displacement of the retaining structure gradually develops downwards during excavation progresses. The maximum uplift of the base is 26.63 mm, and the surface settlement on the cover side of excavation is 60% of that on the open side. The closer the supporting structure is to the bottom of the pit, the greater the change in axial force is as the excavation of the foundation pit.

Keywords: numerical simulation; foundation pit; excavation; deformation; soft soil.

1 Introduction

In recent years, the development of urban underground space has driven subway construction, and foundation pit engineering. As an early stage of underground structures, it faces enormous challenges[1-4]. As the scale and excavation depth of foundation pits increase, the requirements for the use of deep foundation pit engineering are becoming increasingly great. Previous studies mostly focused on the analysis of deformation and stability after excavation of foundation pits. References[5-8] studied the damage of retaining structures in foundation pit caused by stress characteristics, which in turn led to the failure of the entire foundation pit. There is little research on the stress and deformation process of retaining structure and surrounding soil in foundation pit during the entire construction process, especially the deformation of deep foundation pits in soft soil areas and the internal force control of supporting structures.

At present, numerical analysis method[9] and measured data analysis method[10] are mainly used to study the mechanical properties of foundation pit during excavation process. Cheng et al. [11] analyzed the measured data of deformation of the retaining wall, axial force of support and column piles, and surface settlement during the excavation process of a 30.2 m deep foundation pit, then the deformation characteristics of

© The Author(s) 2024

A. E. Abomohra et al. (eds.), *Proceedings of the 2023 9th International Conference on Advances in Energy Resources and Environment Engineering (ICAESSEE 2023)*, Atlantis Highlights in Engineering 29,

https://doi.org/10.2991/978-94-6463-415-0_6

the deep foundation pit during excavation in a specific area of Hangzhou were summarized. The research focuses on the actual excavation steps of each section of the subway deep foundation pit, and the deformation and stress characteristics of the foundation pit and the support structure during the full excavation process were studied. Guidance was provided for practical engineering.

2 Engineering condition

The excavation depth of the foundation pit at Tatou Station is about 17.40 m, the length of the foundation pit is 297.2 m, the width of the foundation pit is from 19.5 m to 27.1 m, and the total length of the station is 297 m.

3 Numerical analysis of the stress and deformation characteristics of covered excavation system in foundation pit

Underground continuous wall and internal support and a combination of concrete support and steel support were adopted as the support form of the foundation pit. MIDAS GTS NX software was used in three-dimensional numerical analysis of foundation pit. The geometric model of the soil in deep foundation pit is shown in Figure 1.

The length, the width and the depth of the model are 390 m, 120 m, and 52 m, respectively. The normal displacement of the model's side and the displacement of the model's bottom in three directions were constrained. The vehicle load on the temporary covered plate of the deep foundation pit with the semi covered excavation method is taken as 20 KPa.

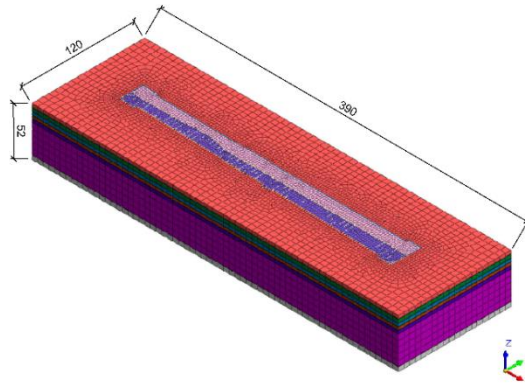


Fig. 1. Geometric model and mesh division of soil (unit: m)

The Mohr-Coulomb constitutive model is applied. A linear elastic constitutive relationship is used for finite element simulation, and the parameters of the numerical calculation model are shown in Table 1.

Table 1. Parameters of support structure in the Model

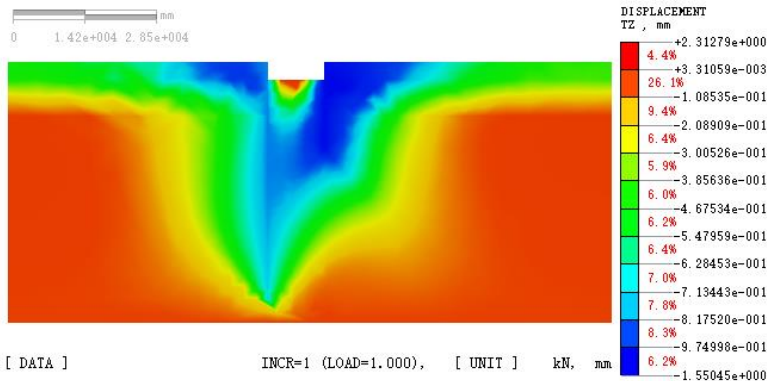
| supporting structure | gravity(kN/m ³) | Elastic modulus(MPa) | Poisson's ratio |
|----------------------------------|-----------------------------|----------------------|-----------------|
| Steel supports, steel pur-lins | 78.5 | 200000 | 0.3 |
| diaphragm wall | 25.0 | 31500 | 0.2 |
| Concrete support and cover plate | 25.0 | 30000 | 0.2 |

3.1 Surface settlement and basement uplift.

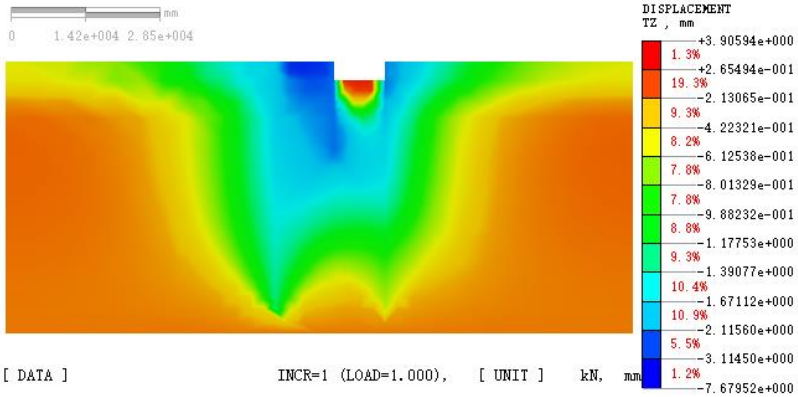
Figure 2 shows the variation of uplift at the bottom of the foundation pit, for the first phase of the foundation pit (Figure 2 (a)), the retaining structure on the south side of the excavation section is stronger than that on the north side. Therefore, the deformation of the upper strata around the south side towards the foundation pit caused by excavation is relatively small, and the offset deformation due to the uplift at the bottom of the pit is relatively small. Therefore, under this working condition, the uplift on the south side of the foundation pit is slightly higher than that on the north side, as the maximum uplift at the bottom of the pit is 2.31 mm.

Under the condition of Phase II, excavation 1 (Figure 2 (b)), the small foundation pit on the covered excavation side has been covered with a cover plate and filled back. The excavation of the first layer of soil on the open excavation side caused the uplift at the bottom of the foundation pit. Due to the limitation of the covered plate on the vertical deformation of the stratum, the uplift on the open excavation side is large on the north side of the foundation pit, as the maximum uplift is 3.9 mm.

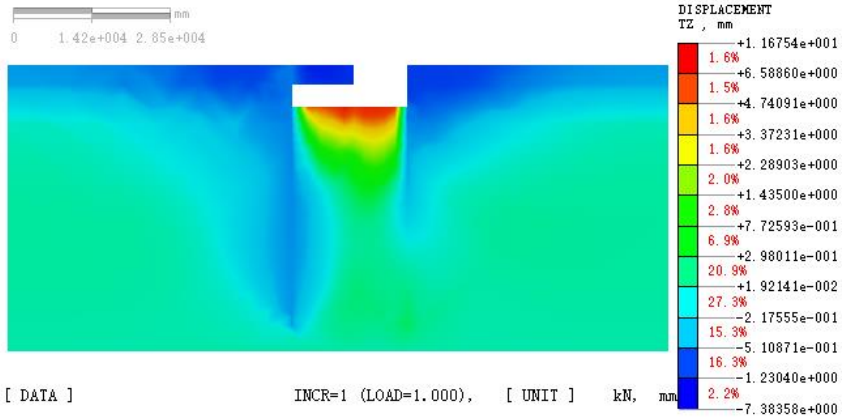
Afterwards (Figure 2 (c)~(f)), as the excavation depth of the foundation pit increases, the soil at the bottom continues to rise upwards, and the uplift gradually increases. It reaches a maximum of 26.63 mm during the excavation of Phase II, foundation pit 5 (excavation of the bottom of the pit). During this period, the uplift deformation of the strata and column piles on the cover excavation side is limited by the upper columns, cover plates, and backfill soil, and the amount of uplift is always smaller than that on the open excavation side.



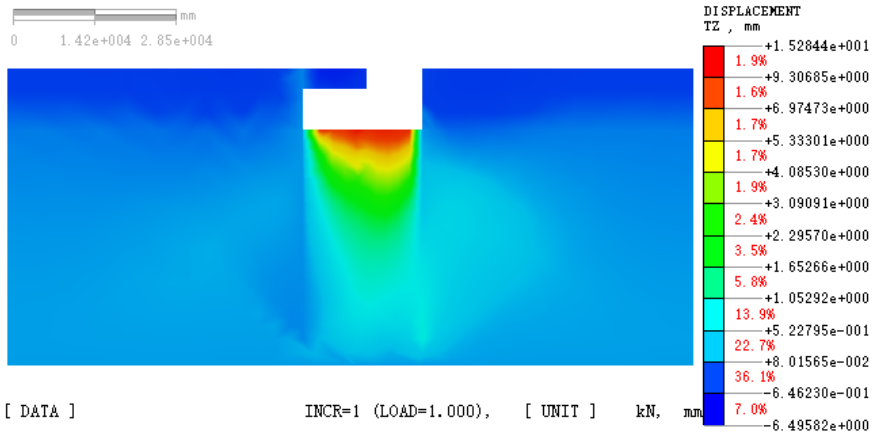
(a)Phase I, excavation



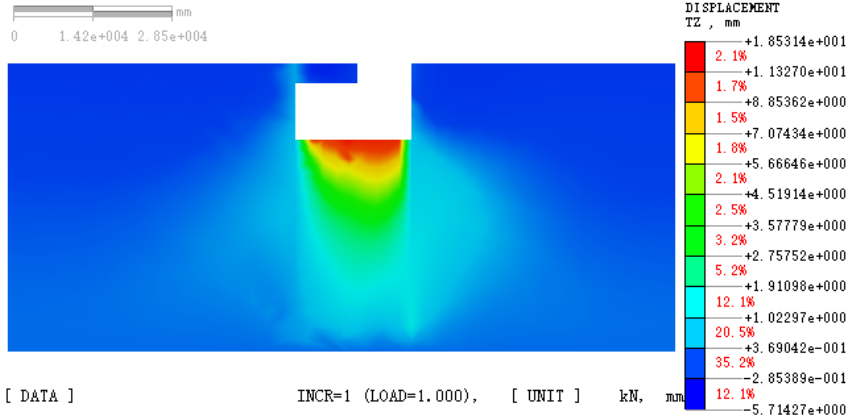
(b)Phase II, excavation 1



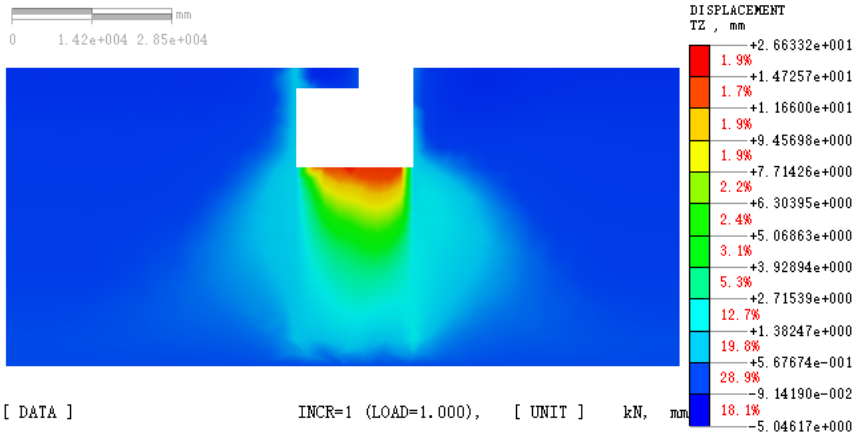
(c) Phase II, excavation 2



(d)Phase II, excavation 3



(e)Phase II, excavation 4



(f)Phase II, excavation 5

Fig. 2. The uplift at the bottom of the foundation pit

Figure 3 shows the surface settlement curve on both sides of the standard section on the foundation pit. It can be seen that the soil near the diaphragm wall on both sides of the foundation pit shows a clear settlement trend, and as excavation proceeds, the settlement gradually increases. In the stable stage after excavation, the value of settlement reaches its maximum, and the settlement of the surrounding surface shows a trend with "groove" shape. Comparing the surface settlement curves on both sides, it can be seen that the lowest point of the groove in the settlement curve on the cover excavation side is closer to the foundation pit, as the distance is 9.65 m and the maximum value of settlement is 5.14 mm. The lowest point on the surface around the open cut side is 14.5 m away from the edge of the foundation pit, and the maximum value of settlement is 8.79 mm.

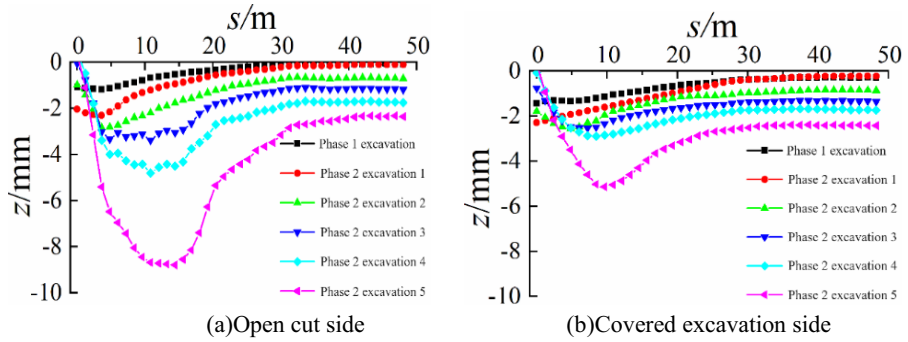


Fig. 3. Surface settlement around both sides of the foundation pit

3.2 Internal force analysis of enclosure structure.

Figure 4 shows the variation trend of supporting axis force during different steps. Seen from Figure 4, when the first concrete support in step 6 was installed, the value of the axial force is 225 kN. After the soil under the support of the next steel support is excavated, the value of axial force increases to 575 kN. After the second steel support is installed, the impact of subsequent excavation steps on the axial force of the first concrete support decreases. After excavating to the location where the fourth support is located, the axial force of the first support reaches a maximum of 700 kN, and then slightly decreases to 677 kN after the excavation of the base.

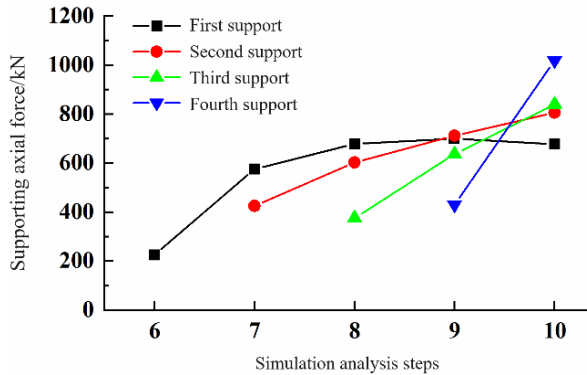


Fig. 4. Supporting axis force under different steps

The axial force with the initial installation of the second, third, and fourth steel supports is around 400kN, which is much greater than the axial force during the initial installation of the first support. Then it rapidly increases with excavation, which reaches its maximum as the bottom of the pit is excavated. The axial force of the fourth support increased fastest, which is followed by the third support. Therefore, the maximum axial force of the steel support occurs on the fourth steel support when the excavation of the foundation pit is completed. The maximum value of axial force is 1019.2 kN, which is less than the controlled value (2000kN).

4 Conclusions

During excavation of deep foundation pit, the deformation and internal force changes of the support system and surrounding soil were analyzed. The conclusions are as follows: the axial force of the internal support is closely related to the vertical layout position of the internal support. The lower the position of the support structure, the greater the axial force of the support structure, which is extremely unfavorable for the support of foundation pit. Therefore, accurate design of positions of concrete support is crucial. As excavation proceeds, the settlement trend of the surrounding ground shows a "groove" shape, and the lowest point of the groove on the settlement curve of the covered excavation side is closer to the foundation pit.

References

1. Mangushev R A, Osokin A I, Garnyk L V. Experience in preserving adjacent buildings during excavation of large foundation pits under conditions of dense development[J]. *Soil Mechanics and Foundation Engineering*, 2016, 53(5): 291-297.
2. Taiyari F, Hajihassani M, Kharghani M. Efficiency of the evolutionary methods on the optimal design of secant pile retaining systems in a deep excavation[J]. *Neural Computing and Applications*, 2022, 34(22): 20313-20325.
3. Taiyari F, Hajihassani M, Kharghani M. Efficiency of the evolutionary methods on the optimal design of secant pile retaining systems in a deep excavation[J]. *Neural Computing and Applications*, 2022, 34(22): 20313-20325.
4. Mangushev R A, Nikiforova N S. Technological settlements of the surrounding buildings during the construction of deep pit fences[J]. *Soil Mechanics and Foundation Engineering*, 2023, 60(1): 15-21.
5. Li F X, Li G Q, Wei X. Affecting factors analysis of stress and deformation of retaining structures in deep excavation pit with weathered granite[J]. *Highways and Automotive Applications*, 2022: 72-77.
6. Chen S R, Cui J F, Liang F Y. Case study on the deformation coupling effect of a deep foundation pit group in a coastal soft soil area[J]. *Applied Sciences-Basel*, 2022, 12(12): 6205.
7. Cheng X S, Zhen J, Zheng G. et al. Research on sliding radius of basal heave failure of excavation in soft soil area[J]. *Journal of Architecture and Civil Engineering*, 2021, 38(6): 90-97. (in Chinese).
8. Zhu D P, Xie C J, Yang Y. Influencing factors of deformation and failure of adjacent buildings induced by deep foundation pit excavation and precipitation[J]. *Science Technology and Engineering*, 2022, 22(3): 1166-1172. (in Chinese).
9. Fen Z Y, Xu Q, Xu X Y, et al. Deformation Characteristics of Soil Layers and Diaphragm Walls during Deep Foundation Pit Excavation: Simulation Verification and Parameter Analysis[J]. *Symmetry-Basel*, 2022, 14(2): 254.
10. Ying X L. Deformation monitoring and numerical simulation analysis of deep foundation pit excavation in soft soil layer [D]. Mianyang: Southwest University of Science and Technology, 2021. (in Chinese).
11. Cheng K, Xu R Q, Ying H W, et al. Performance analysis of a 30.2 m deep-large excavation in Hangzhou soft clay[J]. *Chinese Journal of Rock Mechanics and Engineering*, 2021, 40(4): 851-863. (in Chinese).

Open Access This chapter is licensed under the terms of the Creative Commons Attribution-NonCommercial 4.0 International License (<http://creativecommons.org/licenses/by-nc/4.0/>), which permits any noncommercial use, sharing, adaptation, distribution and reproduction in any medium or format, as long as you give appropriate credit to the original author(s) and the source, provide a link to the Creative Commons license and indicate if changes were made.

The images or other third party material in this chapter are included in the chapter's Creative Commons license, unless indicated otherwise in a credit line to the material. If material is not included in the chapter's Creative Commons license and your intended use is not permitted by statutory regulation or exceeds the permitted use, you will need to obtain permission directly from the copyright holder.

